Int. J. Electron. Commun. (AEÜ) 130 (2021) 153572

Contents lists available at ScienceDirect

International Journal of Electronics and Communications

journal homepage: www.elsevier.com/locate/aeue

Regular paper

Combining designs of precoder and equalizer for MIMO FBMC-OQAM systems based on power allocation strategies

Bui Quoc Doanh [a,c], Do Thanh Quan [b], Ta Chi Hieu [a], Pham Thanh Hiep [a,*]

[a] Faculty of Radio-Electronics Engineering, Le Quy Don Technical University, Hanoi, Viet Nam
[b] Faculty of Technical Command and Staff, Le Quy Don Technical University, Hanoi, Viet Nam
[c] Faculty of Professional Telecommunication, University of Telecommunications, Nhatrang, Viet Nam

ARTICLE INFO

Keywords:
MIMO
FBMC
OQAM
Precoding
Equalization
Prototype filter
Overlapping factor

ABSTRACT

The filter bank multi-carrier (FBMC) technique is hoped to become a potential candidate for advanced wireless multiple intput multiple output (MIMO) systems as the fifth generation (5G) or the sixth generation (6G) owing to its advantages. In this paper, two combining designs of precoder and equalizer for MIMO FBMC offset quadrature amplitude modulation (OQAM) systems are investigated and proposed. These designs are developed basically on power allocation strategies such as the error balance algorithm (EBA) and water-pouring algorithm (WPA). The key idea is how to address bad sub-channels in which they are strengthened with the EBA whereas some really bad sub-channels are discarded with the WPA. The proposed designs are evaluated and compared to outstanding conventional designs based on zero forcing (ZF) and minimum mean square error (MMSE) algorithms via bit error rate (BER) and throughput issues. Simulation results show that the proposed designs can improve significantly the performance of downlink spatial multiplexing systems.

1. Introduction

There has been increasing research on the filter bank multi-carrier (FBMC) technique because it provides some advantages as high spectral efficiency, high data rate, flexible signal processing at receivers, and low side-lobe radiation in comparison to other multi-carrier techniques as orthogonal frequency division multiplexing (OFDM), generalized frequency division multiplexing (GFDM), and universal-filtered multi-carrier (UFMC) [1–5]. Therefore, it may become a potential candidate to apply for advanced wireless systems as the fifth generation (5G) and beyond [6–8] beside other techniques to reduce mutual coupling between perpendicularly placed antennas and design antennas [9–13].

To improve the quality and apply the FBMC technique to advanced wireless systems, a lot of researches investigated and proposed precoding methods, equalization methods, and combining methods of precoding and equalization. These relative outstanding methods are reviewed carefully to illustrate the analysis and contribution of our paper.

Firstly, there were some papers that proposed precoding methods to improve for the FBMC technique when applied to the 5G [14–18]. In [14], the authors investigated a Walsh-Hadamard precoding scheme using the unitary matrix for circular-FBMC, called as WHT-C-FBMC, and an improvement in the system quality was evaluated by providing BER approximation calculation. In [15,16], the authors proposed precoders for a single input and single output (SISO) FMBC system in which they were developed on the basis of zero forcing (ZF) and minimum mean square error (MMSE) criteria. Moreover, a Tomlinson-Harashima precoder was proposed for the down-link of multi-user multiple input and MIMO-FBMC systems in [17], and an effect of channel state information (CSI) was analyzed and evaluated when a precoder based on the ZF criteria was applied to multi-user MIMO-FBMC systems [18]. Some other papers proposed overhearing protocols for MIMO relaying systems and then precoding at relay nodes was optimized under conditions as the minimum weighted mean squared error, maximum weighted sum-rate of all data traffics, and minimum total power [19–21].

Secondly, many designs of equalizers were considered and proposed for FBMC systems in [22–25]. For example, equalizers were analyzed and designed based on ZF and MMSE criterion to improve the BER performance of MIMO-FBMC systems [22]. In [23], designing of equalizer for MIMO-FBMC systems was focused on reducing the effect of channel frequency selectivity by applying geometric transformation interpolation methods. In addition, a decision feedback equalizer based

* Corresponding author.
E-mail addresses: buiquocdoanh@tcu.edu.vn (B.Q. Doanh), dtquan@lqdtu.edu.vn (D.T. Quan), hieunda@mta.edu.vn (T.C. Hieu), phamthanhhiep@gmail.com (P.T. Hiep).

https://doi.org/10.1016/j.aeue.2020.153572
Received 24 August 2020; Accepted 1 December 2020
Available online 19 December 2020
1434-8411/© 2020 Elsevier GmbH. All rights reserved.

on the MMSE criteria was developed to improve the quality of FBMC-OQAM systems in which beside feed-forward and feedback filters, two inter-carrier interference (ICI) filters were added to mitigate ICI from adjacent sub-channels [24]. As a result, while this design had a fairly high complex implementation, it improved significantly the bit error rate (BER) performance due to effective cancellation out inter-symbol Interference (ISI) and ICI even with multi-path fading channels. In [25], the authors developed an equalization technique for MIMO-FBMC OQAM systems by using artificial intelligence. The mean square error (MSE) was trained by a neural network (NN) with the gradient descent algorithm to enhance an estimation and compensation to channel, and simulation results showed that the GN-NN could hang on dynamically the channel, consequently, the channel estimation and compensation were better than that of the least mean square method.

Thirdly, joint designs of precoder and equalizer were proposed for MIMO-FBMC systems to improve spectral efficiency and system quality as in [26–29]. In [26,27], precoders and decoders were designed with ZF and MMSE criterion for MIMO FBMC-OQAM systems under a condition of strong selective fading channels. In [28], two designs of precoders and equalizers based on MMSE and signal-to-leakage ratio were proposed to address limitations of frequency selective channels and an allowed number of receiving antennas at users. In [29], joint designs of MIMO precoding and decoding matrices were proposed under the criteria of minimizing the sum MSE to overcome problems of highly frequently selective channel and support multi-stream transmission.

Finally, in our previous works [30,31], joint designs of precoder and equalizer for ISI MIMO systems were developed basically on shared redundancy, and the effect of imperfect CSI was also taken into account. In this paper, combining designs of precoder and equalizer for MIMO-FBMC OQAM systems are analyzed and developed depending on power allocation strategies such as the error balance and water-pouring algorithms. The key idea is how to treat with bad sub-channels that influence remarkably on the system quality. While bad sub-channels are strengthened in the error balance algorithm, they are discarded in the water-pouring algorithm to save power for other good sub-channels.

The system performance is evaluated by BER and throughput through Monte Carlo simulation programs, and simulation results state that proposed designs can improve significantly the system performance. The proposed designs can be applied in the downlink of spatial multiplexing systems. In some multi-user MIMO systems, each symbol stream may belong to a typical user, as a result, it is necessary to maintain equal error on all streams and then the EBA can be applied. Furthermore, in some applications requiring high data rate as video, the WPA should be applied because it can improve remarkably the system throughput and BER.

The rest of the paper is organized as follows. Section 2 illustrates the system model and background of relative issues as FBMC structure, prototype filter, and OQAM scheme. Section 3 expresses conventional designs of equalizer based on ZF and MMSE criteria, and combining designs of precoder and equalizer based on power allocation strategies. Section 4 provides simulation results and discussions. Finally, Section 5 concludes the paper.

The used notations in this paper are expressed as follows. Matrices and vectors are illustrated by bold lowercase and uppercase letters, respectively. $\Re()$ is real part and $\Im()$ is imaginary part. Let $E(\cdot)$ and $tr(\cdot)$ respectively be the expectation and trace operators. In short, $(\cdot)^*, (\cdot)^H$, and $(\cdot)^T$ describe complex conjugation, Hermitian transpose, and transpose operation, respectively.

2. System model

In this work, a MIMO FBMC-OQAM system that consists of M_T transmitting antennas and M_R receiving antennas is investigated, and some main relative technical issues such as FBMC structure, prototype filter and OQAM scheme are presented shortly.

The proposed system and data streams are shown in Fig. 1. The authors assume that N_c is a sufficient number of sub-carriers corresponding to channel delay spread and each sub-channel can be considered as flat so that precoding and equalization can be performed at any sub-channel. A precoder at the transmitter and a equalizer at the receiver with the i^{th} sub-channel are defined as $\mathbf{F}(\omega_i)$ and $\mathbf{G}(\omega_i), i = 1,2,\ldots,N_c$, respectively. The filter bank consists of synthesis filter bank (SFB) blocks at the transmitter and analysis filter bank (AFB) blocks at the receiver. In the signal processing procedure, input data is firstly transformed by inverse fast fourier transform (IFFT), secondly modulated by the OQAM scheme, thirdly sent to the prototype filter, and finally broadcasted by transmitting antennas in which one antenna will transmit one data stream. At the receiver, the received signals are firstly equalized to cancel ISI, secondly sent to the prototype filter, thirdly transformed by fast fourier transform (FFT), and finally demodulated.

A sub-carrier can be used to transmit S data streams. Besides, the selective frequency fading Rayleigh channel suffered from additive white Gaussian noise (AWGN) is considered in the proposed system. A block of data is transmitted in a time slot. To realize analysis, the channel is assumed to be stable in a time slot but varies in different time slots.

In each time slot, the transmitting antenna sends a block of data that is illustrated as

$$\mathbf{D}_i = [\,a_i \quad b_i\,]^T \tag{1}$$

here $\mathbf{D}_i$ defines a block of data transmitted at the t time slot, and a_i and b_i are datum formed by two input data streams with index i. Moreover, $\mathbf{D}_i$ is also affected by the frequency selective fading Rayleigh channel. In the proposed system, the channel matrix can be demonstrated as

$$\mathbf{H} = \begin{bmatrix} h_{11} & h_{12} \\ h_{21} & h_{22} \end{bmatrix}, \tag{2}$$

here h_{11}, h_{21}, h_{21} and h_{22} are channel factors of four links between transmitter and receiver. In addition, the AWGN that is added to signal sent through the channel is expressed by the following equation

$$\mathbf{n} = [\,n_i \quad \cdots \quad n_n\,]^T. \tag{3}$$

At the channel output, received signals at receiving antennas are described by $\widehat{x}_1$ and $\widehat{x}_2$. It is clear that these signals containing the transmitted signals, AWGN, and ISI are expressed by following equations

$$\widehat{x}_1 = h_{11}a_i + h_{21}b_i, \tag{4}$$

$$\widehat{x}_2 = h_{22}b_i + h_{12}a_i. \tag{5}$$

(4) and (5) can be rewritten as

$$\mathbf{y} = \mathbf{HD} + \mathbf{n} \tag{6}$$

or

$$\begin{bmatrix} \mathbf{y}_1 \\ \mathbf{y}_2 \end{bmatrix} = \begin{bmatrix} h_{11} & h_{12} \\ h_{21} & h_{22} \end{bmatrix} \begin{bmatrix} a_i \\ b_i \end{bmatrix} + \begin{bmatrix} n_1 \\ n_2 \end{bmatrix}. \tag{7}$$

$$\mathbf{y}_1 = h_{11}a_i + h_{21}b_i + n_1 \tag{8}$$

$$\mathbf{y}_2 = h_{22}b_i + h_{12}a_i + n_2. \tag{9}$$

Based on (7), it is possible to process more than one block of data in one time slot by the MIMO system having two transmitting and two receiving antennas.

2.1. FBMC technique

The FBMC can be considered as a typical technique of multi-carrier transmission methods in which filter banks are used at both trans-

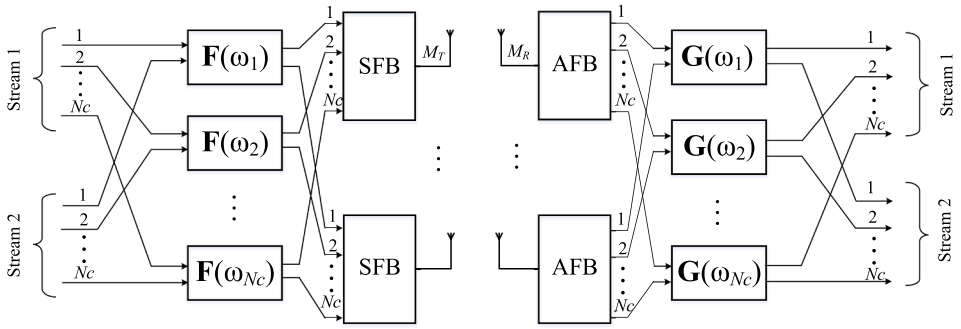

Fig. 1. MIMO FBMC-OQAM system model using joint designs of precoder and equalizer.

mitter and receiver. In the FBMC approach, discrete time transform, IFFT, and FFT are performed effectively when they are combined with SFB scheme at the transmitter and AFB scheme at the receiver [32]. A multi-carrier transceiver employing filter banks can be illustrated as the following equation

$$\mathbf{s}_i(t) = \sum_m \mathbf{s}_i[m]\delta(t - mT). \tag{10}$$

In (10), $\mathbf{s}_i[m]$ are data symbols, i is the sub-carrier index, and T is the symbol period. In this paper, a 4-tap prototype filter provided by PHYDAS [33] is used and $\mathbf{p}_{Tx}$ and $\mathbf{p}_{Rx}$ are denoted for AFB and SFB, respectively. When AFB and FFB are utilized, the signal transmitted via the FBMC system can be expressed as

$$\mathbf{x}(t) = \sum_m \sum_{i=0}^{N_c-1} \mathbf{s}_i[m]\mathbf{p}_{Tx}(t - mT)e^{j2\pi(t-mT)fi}. \tag{11}$$

The signal $\mathbf{x}(t)$ in (11) shows limited time group of complex value of $\mathbf{s}_i[m]$. The period T is always the same with FFT period, however, it maybe less than periods of $\mathbf{p}_{Tx}$ and $\mathbf{p}_{Rx}$, resulting in continuous symbol overlapping. At the transmitter side, a sub-carrier is transmitted through a filter bank $\mathbf{p}_{Tx}$ to form transmitting signal. On the other hand, at the receiver side, a period of $\mathbf{p}_{Rx}$ reduces when signals go through FFT because the period of FFT is equal to versus of distance between frequencies of sub-carriers and it is less than T. Therefore, if the channel is ideal, the received signals $\mathbf{y}(t)$ are totally the same with the transmitted signals $\mathbf{x}(t)$.

2.2. Prototype filter

In the channel multiplexing systems, a prototype filter is a main part in the filter bank because all synthesis and analysis filters are versions with different frequencies in the frequency response of a low-pass prototype filter. As a result, the quality of the filter bank depends significantly on characteristics of the prototype filter. According to the Nyquist theory, the pulse response of a filter used in communication systems has to equal to zero at the end of the period and integer multiple periods. This theory can be applied in the frequency domain based on symmetrical conditions and performed at $1/2$ symbol rate or cut-off frequency. Besides, frequency factors are needed to be considered in the design of filters.

In the transceiver structure, a Nyquist prototype filter is divided into two parts corresponding to transmitter and receiver. The pulse response of a PHYDAS prototype filter [33] with factors of the filter as in Table 1 can be calculated as

$$\mathbf{p}(t) = 1 + 2\sum_{k=1}^{K-1} \mathbf{P}_k \cos\left(2\pi \frac{kt}{KT}\right). \tag{12}$$

The Fig. 2 demonstrates the pulse response of a PHYDAS prototype filter with $N_c = 256$ sub-carriers. The simulation results inform that the pulse response of a filer with $K = 5$ has the maximum amplitude but high values of side-lobe radiations. In cases of $K = 3$ and 4, filters have lower amplitudes, however, they contain lower side-lobe radiations. Some previous works demonstrates that the prototype filter with $K \leqslant 4$ has a good spectrum spread characteristic [34–36], especially, [34] confirms this filter produces the best spectrum efficiency when it is used in the FBMC-OQAM systems.

Table 1
Factors of a prototype filter.

K	P_0	P_1	P_2	P_3	P_4
3	1	0.971960	0.411438	-	-
4	1	0.971960	$\sqrt{2}/2$	0.235147	–
5	1	0.971960	0.88101964	0.4731	0.235147

2.3. OQAM scheme

In FBMC systems, modulation schemes can be applied when sub-carriers are detected. If only either odd index sub-carriers or event index ones are employed, the quadrature amplitude modulation (QAM) scheme can be used because there is no overlapping matter of sub-carriers. However, in order to take the advantage of all sub-carriers to improve transmission rate, the OQAM scheme should be utilized. The reason is that the OQAM scheme can address the overlapping issue of sub-carriers in frequency domain [33]. In this study, the OQAM scheme is used and demonstrated as Fig. 3 [37].

The Fig. 3 illustrates the model of the parallel data transmission system in which sections in the filter bank are assumed to be the same and independently distributed. The sections used in the filter bank can be considered as different versions of time–frequency shifted prototype pulse $p(t)$. The parallel transmission means dividing the total bandwidth into N_c sub-bands and the gap between two continuous sub-carriers is Δ_f. With each sub-carrier, symbols are performed by $p(t)$ and

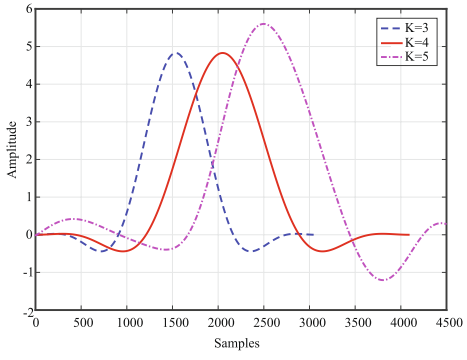

Fig. 2. The pulse response of prototype filters with overlapping factors $K = 3$, 4 and 5.

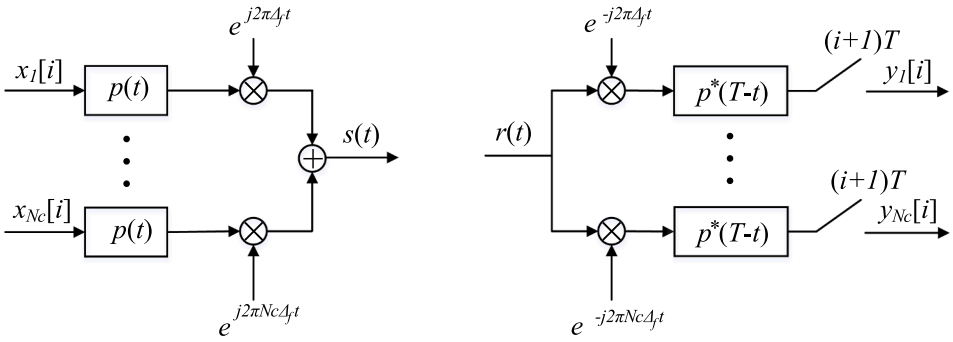

Fig. 3. The parallel data transmission system model.

transmitted by the rate $\frac{1}{T}$, where T is the period of the symbol. The matched filters are formed from $p^*(T-t)$ based on time-shifting and instant sampling at $(k+1)T$ point. Since $p(t)$ is the limited-bandwidth low-pass filter, this method allows the system has an effective controlling of a limited spectrum. In fact, to simply waveform design and enhance spectral efficiency, the roll-off factor is chosen to be higher than zero and spectral overlapping is allowed. The Fig. 3 states that data can be recovered with the ideal channel only if the following equation is satisfied

$$\int p(t-iT)e^{j2\pi m\Delta_f t}\times p^*(t-i')e^{-j2\pi m\Delta_f t}dt = \delta_{i',i}\delta_{m',m}. \tag{13}$$

(13) is the orthogonal condition that requires the data symbol density must satisfy $\frac{1}{\Delta_f T}\leqslant 1$. A prototype pulse satisfies this condition corresponding to the minimum distance between symbols and it is impossible to define symbols in both time and frequency domains [38]. However, the exact location of symbols in both time and frequency domain at $\frac{1}{\Delta_f T}=1$ can be performed if the OQAM scheme is used, and data is alternatively shifted and parallel transmitted corresponding to pulse amplitude modulation (PAM) symbols rate at $(2/T)$ and phase $(\pi/2)$ [39].

In this paper, data symbols are taken from the real value of the PAM constellation. As a result, the symbol rate will be double, in other words, the density of data symbols taken from QAM will be quadruple [40]. However, in comparison to the QAM, the PAM symbol consists of a half of information so that the PAM transmission can provide a twice data symbol density of the QAM transmission. For a detailed explanation, the transmitted signals are expressed in the following equation

$$\mathbf{x}(t) = \sum_m \sum_{i=0}^{N_c-1} \mathbf{s}_i[m]\mathbf{p}_i(t-mT/2) \tag{14}$$

where $\mathbf{s}_i[m]$is data symbol with real value, and $\mathbf{p}_i$ is calculated as the following equation

$$\mathbf{p}_i(t) = \mathbf{p}(t)e^{j\pi iFt}\theta \tag{15}$$

where θ is defined as

$$\theta = e^{j(i+m)\pi/2}. \tag{16}$$

The Fig. 4 demonstrates the process to form OQAM chains based on phase shifting and the QAM symbols $x_m[i]$. The orthogonal condition to totally recover symbols $d_m[i]$ at the receiver is illustrated by the following equation

$$\Re\left(\int p\left(t-i\frac{T}{2}\right)e^{j2\pi m\Delta_f t}\phi_m[i] \times p^*\left(t-i\frac{T}{2}\right)e^{-j2\pi m'\Delta_f t}\phi^*_{m'}[i']dt\right) = \delta_{i',i}\delta_{m',m} \tag{17}$$

here $\phi_m$is the shifted-phase of the m sub-carrier and is defined as

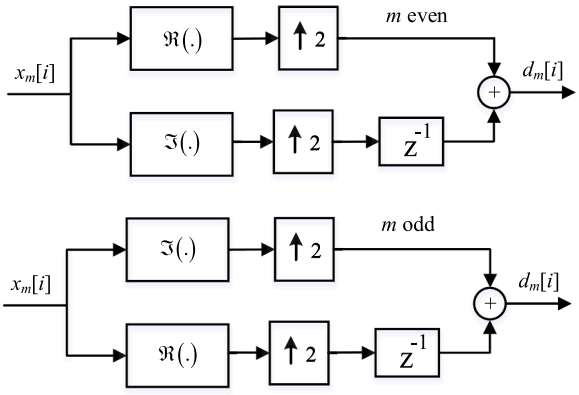

Fig. 4. OQAM in multi-carrier structure.

$$\phi_m[i] = e^{j\left(\frac{\pi}{2}(m+i)-\pi mi\right)} \tag{18}$$

and $\delta_{i,m}$ is the delta Kronecker function expressed by

$$\delta_{i,m} = \begin{cases} 1, & i=m, \\ 0, & i\neq m \end{cases}. \tag{19}$$

In case $(i+m)$ is even, the phase shifting is integer multiple of π, remaining the real value of PAM symbols. On the other hand, in case $(i+m)$ is odd, the phase shifting is the odd-integer multiple of $\pi/2$, converting the real value of PAM symbols into the image value. The phase shifting is made by prototype filters at the transmitter $\mathbf{p}_{Tx}/\mathbf{p}_{Tx}(t-T/2)$ and receiver $\mathbf{p}_{Rx}/\mathbf{p}_{Rx}(t-T/2)$.

3. Combining designs of precoder and equalizer for MIMO FBMC systems

3.1. Designs of equalizers based on conventional ZF and MMSE algorithms

There are two basic linear equalization methods, the ZF and MMSE. The ZF equalizer uses an inverse filter at the receiver to coerce the influence of the channel response. It means that the entire channel response of one output symbol will be separated and the other symbols response equals to zero.

Considering a MIMO-FBMC system with the same number of transmitting and receiving antennas, the **H**-channel matrix is a square matrix with the rank is equal to the number of transmitting or receiving antennas and there is an inverse matrix at the receiver. Applying the inverse impulse response of the channel, Eq. (6) can be presented as

$$\mathbf{y}\mathbf{H}^{-1} = \mathbf{D} + \mathbf{n}\mathbf{H}^{-1}. \tag{20}$$

When using the ZF equalizer to separate data symbols, a $\mathbf{Z}_{ZF}$ matrix that satisfies $\mathbf{Z}_{ZF}\mathbf{H} = \mathbf{I}$ is required. This condition is achieved by using an inverse matrix at the receiver and is calculated as

$$\mathbf{Z}_{ZF} = \left[\mathbf{H}^H\mathbf{H}\right]^{-1}\mathbf{H}^H. \tag{21}$$

Unlike the ZF equalizer, the MMSE equalizer is not greatly influenced by the noise amplification effect because the MMSE equalizer takes into account the characteristics of the noise. Therefore, the MMSE method always provides better BER quality than the ZF method. Although the MMSE method is as simple as the ZF method, the MMSE method is considered as one of the good methods to eliminate noise. In fact, the MMSE method does not completely eliminate noise. Instead, there is a trade-off between the cancellation of ISI noise and the noise power of the received signal. Similar to the ZF method, we can calculate the MMSE equalization matrix as

$$\mathbf{Z}_{MMSE} = \left[\mathbf{H}^H\mathbf{H} + \sigma_g^2\mathbf{I}\right]^{-1}\mathbf{H}^H. \tag{22}$$

It is easy to see that the MMSE equalization matrix is only different from the ZF equalization matrix in a noise power component σ_g^2 or SNR. Therefore, Eq. (22) can be rewritten as

$$\mathbf{Z}_{MMSE} = \left[\mathbf{H}^H\mathbf{H} + \frac{1}{SNR}\mathbf{I}\right]^{-1}\mathbf{H}^H. \tag{23}$$

Although both the ZF and MMSE methods significantly improve the transmission efficiency of the MIMO FBMC system, these two methods will become ineffective in processing ISI if the transmission power is limited. In this case, the energy levels on the sub-channels are very different, especially, when the sub-channels have low eigenvalues. This causes some signals on sub-channels with low eigenvalues to be unable to transmit to the receiver, resulting in a decrease in transmission efficiency.

3.2. A combining design based on the error balance algorithm

To overcome the above disadvantages, the paper proposes a design combining a precoder $\mathbf{F}$ on the transmitter side and a $\mathbf{G}$ equalizer on the receiver side. According to this design, Eq. (6) can be rewritten as

$$\mathbf{y} = \mathbf{GHFD} + \mathbf{Gn}. \tag{24}$$

Considering the condition of the transmission power p_0 for all sub-carrier waves is constrained. To optimize precoding and equalization matrices for the MIMO FBMC system with fixed input data streams S. The precoder and equalizer must be designed to ensure SNR balance or to provide equal error probability on each sub-carrier wave. Applying the formula for calculating the probability of balancing errors on sub-channels [41], this design is carried out according to the weight equation as

$$\mathbf{W}^{1/2}\mu^{-1/2}\mathbf{\Lambda}^{1/2} - \mathbf{I} = \gamma\mathbf{I} \tag{25}$$

where $\mathbf{W}$ is a positive diagonal weight matrix and $\mathbf{\Lambda}$ is the diagonal matrix whose diagonal elements are calculated by the real number part of singular value decomposition analysis which uses the following equation

$$\mathbf{H}^H\mathbf{R}_\mathbf{n}^{-1}\mathbf{H} = \mathbf{V}\Lambda\mathbf{V}^H \tag{26}$$

and $\gamma$is a scalar value. From (25), the weight matrix $\mathbf{W}$ is rewritten as follows:

$$\mathbf{W}^{1/2} = (1+\gamma)\mathbf{\Lambda}^{-1/2}\mu^{1/2} \tag{27}$$

where $\mu$is a function of $\mathbf{W}$ and is optimized by the method of Lagrange multipliers

$$\mu^{1/2} = \frac{tr\left(\mathbf{\Lambda}^{-1/2}\mathbf{W}^{1/2}\right)}{tr(\mathbf{\Lambda}^{-1}) + \rho_0}. \tag{28}$$

Substituting the value of μ from (27) into (28), γ is calculated as

$$\gamma = \frac{p_0}{\mathrm{tr}(\mathbf{\Lambda}^{-1})}. \tag{29}$$

Substituting the value of γ into (27), we evaluate the weight matrix $\mathbf{W}$ as

$$\mathbf{W}^{1/2} = \mu^{1/2}\left(\frac{\rho_0}{tr(\mathbf{\Lambda}^{-1})} + 1\right)\mathbf{\Lambda}^{-1/2}. \tag{30}$$

The elements on the main diagonal of matrices $\mathbf{\Phi}_\mathrm{f}$ and $\mathbf{\Phi}_\mathrm{g}$ are optimized by the method of Lagrange multipliers

$$\mathbf{\Phi}_\mathrm{f} = \left(\mu^{-1/2}\mathbf{\Lambda}^{-1/2}\mathbf{W}^{1/2} - \mathbf{\Lambda}^{-1}\right)_+^{1/2} \tag{31}$$

$$\mathbf{\Phi}_\mathrm{g} = \left(\mu^{1/2}\mathbf{\Lambda}^{-1/2}\mathbf{W}^{-1/2} - \mu\mathbf{\Lambda}^{-1}\mathbf{W}^{-1}\right)_+^{1/2}\mathbf{\Lambda}^{-1/2} \tag{32}$$

where $()_+$ character refers to the negative components of the diagonal matrix in parentheses that will be replaced with 0.

Substituting the value of $\mathbf{W}$ from Eq. (30) into (31) and (32), we can calculate values of elements on the main diagonal of two matrices $\mathbf{\Phi}_\mathrm{f}$ and $\mathbf{\Phi}_\mathrm{g}$ as

$$\mathbf{\Phi}_\mathrm{f} = \gamma^{1/2}\mathbf{\Lambda}^{-1/2} \tag{33}$$

$$\mathbf{\Phi}_\mathrm{g} = \gamma^{1/2}(1+\gamma)^{-1}\mathbf{\Lambda}^{-1/2}. \tag{34}$$

As a result, when the transmission power is divided equally on each sub-carrier wave, the precoding matrix $\mathbf{F}$ and equalization matrix $\mathbf{G}$ are calculated as

$$\mathbf{F} = \mathbf{V}\mathbf{\Phi}_\mathrm{f}, \tag{35}$$

$$\mathbf{G} = \mathbf{\Phi}_\mathrm{g}\mathbf{V}^H\mathbf{H}^H\mathbf{R}_\mathbf{n}^{-1} \tag{36}$$

where $\mathbf{R}_\mathbf{n}$ is the noise covariance matrix and $\mathbf{V}$ is the unitary matrix calculated by (26).

From the value of γ in (29), we see that the power distribution on the sub-channels is equal. This means that, with this design, sub-channels with low eigenvalues will be allocated more power, otherwise sub-channels with high-eigenvalues will be allocated less power. This results in the equality of SNR and MSE on each sub-channel. According to this design, some sub-channels with low eigenvalues will not be eliminated, therefore, the BER quality has been improved in comparison to previous designs.

3.3. A combining design based on the water-pouring algorithm

The proposed design based on the error balance algorithm as in the previous section is developed with the main idea is that the power is distributed equally on sub-channels, in other words, there is a fair treatment between good sub-channels and bad sub-channels. As a result, the SERs of symbol streams or capacities of sub-channels are balanced. However, there is another positive way to address the bad sub-channels that is to discard really bad sub-channels and then save obtained power to re-distribute to better sub-channels. This method is to use the water-pouring algorithm in the power allocation strategy for sub-channels. In this section, we will propose a combined design based on the water-pouring power allocation algorithm. This design may improve the throughput and quality of some typical MIMO FBMC systems.

The design based on the water-pouring algorithm is performed by a selection of weight values in (25) as $\mathbf{W} = \mathbf{I}$. Therefore, elements on diagonals of $\mathbf{\Phi}_\mathrm{f}$ matrix and $\mathbf{\Phi}_\mathrm{g}$ are optimized by the method of Lagrange multipliers

$$\mathbf{\Phi}_{\mathrm{f}} = \left(\mu^{-1/2}\mathbf{\Lambda}^{-1/2} - \mathbf{\Lambda}^{-1}\right)_{+}^{1/2} \tag{37}$$

$$\mathbf{\Phi}_{\mathrm{g}} = \left(\mu^{1/2}\mathbf{\Lambda}^{-1/2} - \mu\mathbf{\Lambda}^{-1}\right)_{+}^{1/2}\mathbf{\Lambda}^{-1/2} \tag{38}$$

where $\mathbf{\Lambda}$ is defined as in (26) and $\mu$is illustrated as in (28) and represented as

$$\mu^{1/2} = \frac{tr\left(\mathbf{\Lambda}^{-1/2}\right)}{tr(\mathbf{\Lambda}^{-1}) + \rho_0}. \tag{39}$$

Setting $\mathbf{\Lambda} = diag(\lambda_1, \lambda_2, \ldots, \lambda_B)$ where λ values are ordered decreasingly as $\lambda_1 \geqslant \ldots \geqslant \lambda_k \geqslant \ldots \geqslant \lambda_B$. In this paper, the transmission power is assumed to be constrained, $tr(\mathbf{\Phi}_f^2) = \rho_0$. When the number of sub-channels k satisfies $k \leqslant B$, where $B = rank(\mathbf{H})$, the expression of μ in (39) can be rewritten as

$$\mu^{1/2} = \frac{\sum_{i=1}^{k}\left(\lambda_i^{-1/2}\right)}{p_0 + \sum_{i=1}^{k}(\lambda_i^{-1})}. \tag{40}$$

Let $\mathbf{\Phi}_{\mathrm{f}} = diag(\left[\phi_{f1}, \phi_{f2}, \ldots, \phi_{fB}\right])$. The repeating process is set with $k = B$ to calculate $\mathbf{\Phi}_{\mathrm{f}}$. As a result, the power allocation strategy is performed as following steps.

Step 1: Suppose that $\mu \leqslant \lambda_k$. From (37), applying $\phi_{f,i} \geqslant 0$, with $i = 1, 2, \ldots, k$, the value of μ is calculated in this scenario. The procedure operates in the condition $\mu \leqslant \lambda_k$; otherwise, stop and go to step 2.

Step 2: Set $\phi_{j,k} = 0$ and $k = k - 1$, and then come back to the Step 1.

It is clear that after each loop, the transmission power is re-distributed to a sub-channel with higher eigenvalue in the set of sub-channels. Since there are B eigenvalues, the repeating process is completed at the $B-1$ stage. In this process, the transmission power is concentrated on sub-channels with highest eigenvalue.

Different from the proposed design based on the error balance algorithm, the transmission power is re-distributed many times in the design based on the water-pouring algorithm. Moreover, there are also different strategies to treat with bad sub-channels corresponding to low eigenvalues between two designs. While bad sub-channels are treated fairly in the design based on the error balance algorithm, they are distributed less power, even though, some really bad sub-channels are discarded and then obtained power is provided to good sub-channels.

4. Simulation results

In this paper, two combining designs of precoder and equalizer based on the EBA and the WPA in the power allocation strategy are proposed. To demonstrate research results, the Monte Carlo simulation is developed to evaluate and compare these two proposed designs with two conventional designs based on the MMSE and ZF [22] via BER and throughput issues. Some parameters are set as follows. The modulation scheme is OQAM, the fading Rayleigh channel is assumed to be changed slowly and considered as flat at a sub-channel, the number of sub-channels is $N_c = 256$, and the total transmission power is constrained and normalized as $p_0 = 1$.

As can be seen from Fig. 5, the BER performance of systems used the EBA design, and conventional ZF and MMSE designs [22] are compared in case the number of transmitting antennas and receiving ones are equal to 2, and the overlapping factor K is 3. It is clear that the BER performance of the system utilized the EBA design is significantly better than that used ZF and MMSE designs. For example, at the same SNR is 25 dB, the BER of systems employed EBA, MMSE and ZF are 2.10^{-5}, 8.10^{-4} and 6.10^{-3}, respectively. Moreover, the gaps between curves increase when the SNR rises and the BER performance of the system used the ZF designs is worst.

There are some main reasons to explain the above simulation results.

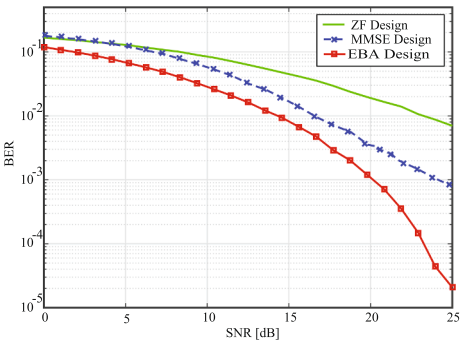

Fig. 5. A BER comparison of EBA, MMSE and ZF designs with $M_T = M_R = 2$ and $K = 3$.

Firstly, since the ZF design uses the inverse filter to address the impact of channel response and the MMSE design takes into account the noise characteristic, the MMSE design is suffered less significantly by the effect of noise amplitude than the ZF design. Moreover, while these two designs have almost the same computing complex, the MMSE design can cancel noise more efficiently than the ZF one. Consequently, the MMSE design frequently provides better BER performance than the ZF one. Secondly, there is a trade-off between the noise cancellation ability and transmission power in the MMSE and ZF designs. As a result, if the transmission power is constrained, these tow designs are low effective when they are applied to the MIMO FBMC system. Thirdly, the transmission power allocation strategy of the EBA design is more effective than that of the MMSE and ZF designs. The distributed power of sub-channels in the MMSE and ZF designs is really different, especially, some bad sub-channels with low eigenvalues usually get low power and can not support to send signals to a receiver. In contrast, bad sub-channels are distributed power fairly in the EBA design and then they can contribute to the signal broadcasting.

In the Figs. 6 and 7, while the overlapping factor is changed, $K = 4$ and $K = 5$, other parameters are keep stable. It is obvious that the EBA design provides a remarkable improvement to the quality of the MIMO FBMC system in comparison with the MMSE and ZF designs. The trend of curves is almost the same as that of the Fig. 5, demonstrating the value of the proposed method. Furthermore, the EBA designs with different overlapping factors, $K = 3, K = 4$, and $K = 5$ are compared in the Fig. 8. The simulation results show that the optimal overlapping factor is 4 and this finding meets the same conclusion as proof in [34]. In the FBMC system, the performance of the system depends on the characteristics of the sample filter. As described in Fig. 2, in the case of the sample filter with overlapping factor $K = 5$, despite having the largest pulse response amplitude, out-of-band ripples are the largest. In the case of the sample filter with $K = 3$, although the pulse response amplitude is smaller than that in the case of $K = 5$, the out-of-band ripples are smaller. Therefore,

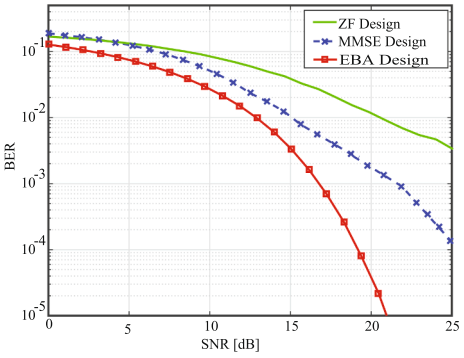

Fig. 6. A BER comparison of EBA, MMSE and ZF designs with $M_T = M_R = 2$ and $K = 4$.

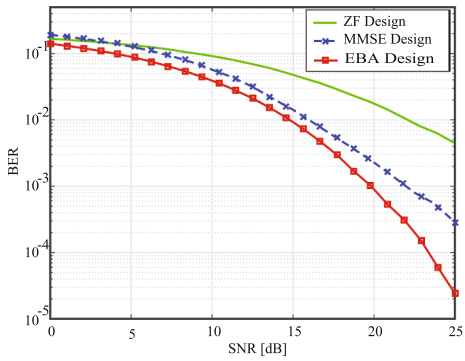

Fig. 7. A BER comparison of EBA, MMSE and ZF designs with $M_T = M_R = 2$ and $K = 5$.

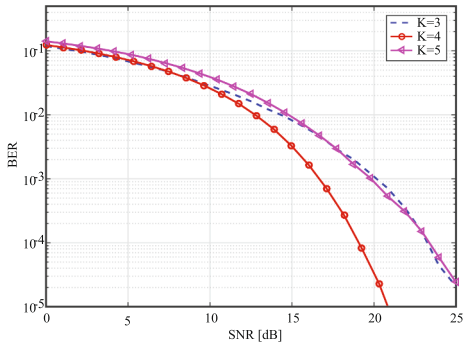

Fig. 8. A BER comparison between EBA designs with $M_T = M_R = 2$ and $K = 3,4,5$.

the BER of the MIMO FBMC system of these two cases is almost equal. Meanwhile, the sample filter with overlapping factor $K = 4$gives the best spread spectrum properties, consequently, the BER of the MIMO FBMC system in this case is the lowest.

In the Fig. 9, three designs are evaluated when the number of antenna increases and the optimal overlapping factor is chosen, $M_T = M_R = 4$ and $K = 4$. The Fig. shows that the EBA design has the best BER performance while the ZF design has the worst one. In addition, a comparison between the Fig. 6 and 9 informs that when the number of antennas rises, the BER performance of designs decreases, and the gap between curves declines as well. This issue is explained as when the number of antennas goes up, the number of sub-channels increases, and then the effect of bad sub-channels becomes worse in all three designs due to the constrained transmission power. Therefore, the total BER of all symbol streams increases or the system quality goes down. Moreover, when the SNR is low (SNR less than 15 dB), the energy distribution on the sub-channels does not differ greatly, and then the BER performance of MMSE and EBA designs is almost the same and two corresponding curves overlap in this region. However, when the SNR value increases (greater than 15 dB), the energy distribution on the sub-channels is more different. As a result, a few sub-channels may have really low power, the EBA design shows a significant improvement and the gaps between curves increase remarkably.

In short, two proposed designs, EBA and WPA, and the MMSE design are analyzed and compared as in the Fig. 10 and 11. In three designs, the WPA design provides the best quality while the MMSE design has the worst one in both BER and throughput issues. Moreover, since gaps between curves are really large, it states that the WPA can improve remarkably the system quality. For instance, in order to archive the BER at 2.10^{-3}, required SNRs of the WPA, EBA, and MMSE designs are 8, 15 and 20 dB, respectively, in other words, the obtained gain of the WPA design in comparison with two other designs are 7 and 12 dB. This improvement can be demonstrated in the following reason. In the WPA design, the transmission power is distributed basically to good sub-channels and then the effect of bad sub-channels on the system quality is weakened. Especially, in the WPA design, when the number of antennas increases as illustrated in Fig. 12, the system quality improves also, which is much different from the EBA, MMSE, and ZF designs. The reason is that when increasing the number of antennas or sub-channels, the transmission power is focused more significantly on good sub-channels, and even some bad sub-channels are discarded and the obtained power is re-allocated to good sub-channels. However, in all 4 designs that are analyzed in this paper, the WPA design has the most complex implementation.

5. Conclusion

In this paper, combining designs of precoder and equalizer are analyzed and proposed for the MIMO FBMC-OQAM system corresponding to different power allocation strategies as the error balance algorithm and water-pouring algorithm. The simulation results demonstrate significant improvements that are produced when proposed designs are applied. Moreover, the design based on the water-pouring algorithm shows the best quality but has the most complex implementation, and the optimal overlapping factor for prototype PHYDAS filter is 4. In general, the FBMC technique may become a potential candidate for advanced wireless MIMO systems such as 5G or 6G because of its advantages. However, in comparison to the conventional OFDM technique, the FBMC technique has a higher complex implementation, especially in the overlapping matter between sub-channels and synchronization of prototype filters in de/multiplexing signals. Moreover, the proposed methods in this study can be applied for MIMO systems used other multi-carrier techniques as OFDM, GFDM, and UFMC. These issues will be left to the future work of the paper.

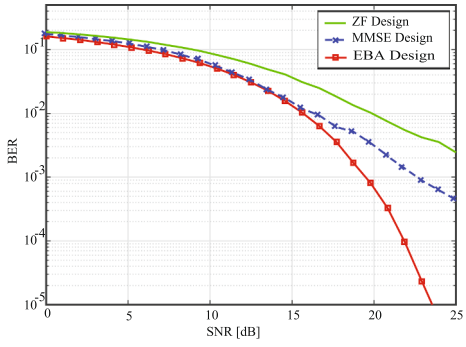

Fig. 9. A BER comparison of EBA, MMSE and ZF designs with $M_T = M_R = 4$ and $K = 4$.

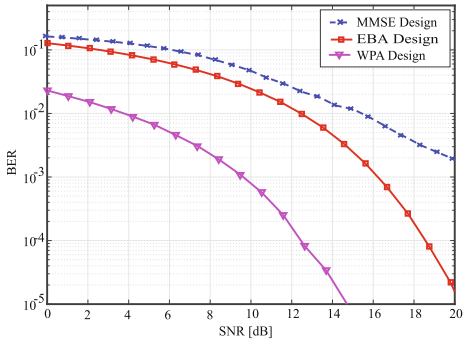

Fig. 10. A BER comparison of WPA, EBA and MMSE designs with $M_T = M_R = 2$.

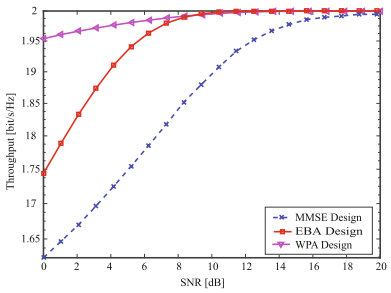

Fig. 11. A throughput comparison of WPA, EBA and MMSE designs with $M_T = M_R = 2$.

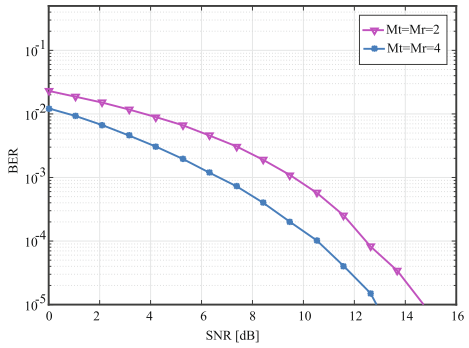

Fig. 12. A BER comparison between WPA designs corresponding to $M_T = M_R = 2$ and $M_T = M_R = 4$.

Declaration of Competing Interest

The authors declare that they have no known competing financial interests or personal relationships that could have appeared to influence the work reported in this paper.

Appendix A. Supplementary material

Supplementary data associated with this article can be found, in the online version, at https://doi.org/10.1016/j.aeue.2020.153572.

References

[1] Trivedi VK, Ramadan K, Kumar P, Dessouky MI, Abd El-Samie FE. Enhanced OFDM-NOMA for next generation wireless communication: a study of PAPR reduction and sensitivity to CFO and estimation errors. AEU-Int J AEU-Int J Electron Commun 2019;102:9–24.
[2] Ramadan K, Dessouky MI, Abd El-Samie FE. A modified OFDM configuration with equalization and CFO compensation for performance enhancement of OFDM communication systems. AEU-Int J Electron Commun 2020:153247.
[3] Bandari SK, Vakamulla VM, Drosopoulos A. PAPR analysis of wavelet based multitaper GFDM system. AEU-Int J Electron Commun 2017;76:166–74.
[4] Chang Y-K, Ueng F-B. A novel turbo GFDM-IM receiver for MIMO communications. AEU-Int J Electron Commun 2018;87:22–32.
[5] Zerhouni K, Elassali R, Elbahhar F, Elbaamrani K, Idboufker N. On the cyclostationarity of universal filtered multi-carrier UFMC. AEU-Int J Electron Commun 2018;89:174–80.
[6] Nadal J, Nour CA, Baghdadi A. Flexible and efficient hardware platform and architectures for waveform design and proof-of-concept in the context of 5G. AEU-Int J Electron Commun 2018;97:85–93.
[7] Chowdhury MZ, Shahjalal M, Ahmed S, Jang YM. 6G wireless communication systems: Applications, requirements, technologies, challenges, and research directions. IEEE Open J Commun Soc 2020;1:957–75.
[8] Akyildiz IF, Kak A, Nie S. "6G and beyond: The future of wireless communications systems." IEEE Access, vol. 8; 2020. p. 133 995–134 030.
[9] Alibakhshikenari M, Virdee BS, Shukla P, See CH, Abd-Alhameed RA, Falcone F, Quazzane K, Limiti E. Isolation enhancement of densely packed array antennas with periodic MTM-photonic bandgap for sar and MIMO systems. IET Microwaves, Antennas Propag 2019;14(3):183–8.
[10] Alibakhshikenari M, Khalily M, Virdee BS, See CH, Abd-Alhameed RA, Limiti E. "Mutual-coupling isolation using embedded metamaterial EM bandgap decoupling slab for densely packed array antennas." IEEE Access, vol. 7; 2019. p. 51 827–51 840.
[11] Alibakhshikenari M, Khalily M, Virdee BS, See CH, Abd-Alhameed RA, Limiti E. "Mutual coupling suppression between two closely placed microstrip patches using EM-bandgap metamaterial fractal loading." IEEE Access, vol. 7; 2019. p. 23 606–23 614.
[12] Alibakhshikenari M, Virdee BS, Shukla P, See CH, Abd-Alhameed R, Khalily M, Falcone F, Limiti E. Antenna mutual coupling suppression over wideband using embedded periphery slot for antenna arrays. Electronics 2018;7(9):198.
[13] Iqbal A, Saraereh OA, Ahmad AW, Bashir S. Mutual coupling reduction using F-shaped stubs in uwb-mimo antenna. IEEE Access 2017;6:2755–9.
[14] Duong Q, Nguyen HH. "Walsh-hadamard precoded circular filterbank multicarrier communications." In: 2017 International Conference on Recent Advances in Signal Processing, Telecommunications & Computing (SigTelCom). IEEE; 2017. p. 193–8.
[15] Chang BS, da Rocha CA, Le Ruyet D, Roviras D. "On the effect of ISI in the error performance of precoded FBMC/OQAM systems." In: 2012 18th Asia-Pacific Conference on Communications (APCC). IEEE; 2012. p. 987–91.
[16] Chang BS, Da Rocha C, Le Ruyet D, Roviras D. On the use of precoding in FBMC/OQAM systems. In: ITS 2010; 2010.
[17] Cheng Y, Ramireddy V, Haardt M. Non-linear precoding for the downlink of FBMC, OQAM based multi-user MIMO systems. In: WSA 2015; 19th International ITG Workshop on Smart Antennas. VDE; 2015. p. 1–6.
[18] Le Ruyet D, Zakaria R, Özbek B. "On precoding MIMO-FBMC with imperfect channel state information at the transmitter." In: 2014 11th International symposium on wireless communications systems (ISWCS). IEEE; 2014. p. 808–12.
[19] Li C, Wang J, Zheng F-C, Cioffi JM, Yang L. Overhearing-based co-operation for two-cell network with asymmetric uplink-downlink traffics. IEEE Trans Signal Inform Process over Networks 2016;2(3):350–61.
[20] Li C, Yang HJ, Sun F, Cioffi JM, Yang L. Multiuser overhearing for cooperative two-way multiantenna relays. IEEE Trans Veh Technol 2015;65(5):3796–802.
[21] Li C, Zhang S, Liu P, Sun F, Cioffi JM, Yang L. Overhearing protocol design exploiting intercell interference in cooperative green networks. IEEE Trans Veh Technol 2015;65(1):441–6.
[22] Basheer A, Habib A. "Filter bank multi carrier based MIMO system for 5G wireless communication." In: 2016 1st International workshop on link-and system level simulations (IWSLS). IEEE; 2016. p. 1–6.
[23] Da Rocha CAF, Bellanger MG. "Sub-channel equalizer design based on geometric interpolation for FBMC/OQAM systems." In: 2011 IEEE International symposium of circuits and systems (ISCAS). IEEE; 2011. p. 1279–82.
[24] Chen CW, Maehara F. "An enhanced MMSE subchannel decision feedback equalizer with ICI suppression for FBMC/OQAM systems." In: 2017 International conference on computing, networking and communications (ICNC). IEEE; 2017. p. 1041–5.
[25] Waseem A, Khaliq A, Ahmad R, Munir MF. Channel equalization for MIMO-FBMC systems. In: 2016 International Conference on Intelligent Systems Engineering (ICISE); 2016. p. 272–7.
[26] Rottenberg F, Mestre X, Horlin F, Louveaux J. Single-tap precoders and decoders for multiuser MIMO FBMC-OQAM under strong channel frequency selectivity. IEEE Trans Signal Process 2016;65(3):587–600.
[27] Pérez-Neira AI, Caus M, Zakaria R, Le Ruyet D, Kofidis E, Haardt M, Mestre X, Cheng Y. MIMO signal processing in offset-QAM based filter bank multicarrier systems. IEEE Trans Signal Process 2016;64(21):5733–62.
[28] Cheng Y, Baltar LG, Haardt M, Nossek JA. "Precoder and equalizer design for multi-user MIMO FBMC/OQAM with highly frequency selective channels." In: 2015 IEEE international conference on acoustics, speech and signal processing (ICASSP). IEEE; 2015. p. 2429–33.
[29] Caus M, Pérez-Neira AI. Multi-stream transmission for highly frequency selective channels in MIMO-FBMC/OQAM systems. IEEE Trans Signal Process 2013;62(4):786–96.
[30] Doanh BQ, Quan DT, Hiep PT, Hieu TC. A combining design of precoder and equalizer based on shared redundancy to improve performance of ISI MIMO systems. Wirel Netw Jul. 2019;25(5):2741–50.
[31] Doanh BQ, Hieu TC, Hiep PT, Nam TS, Anh PTP. Performance Analysis of Joint Precoding and Equalization Design with Shared Redundancy for Imperfect CSI MIMO Systems. Adv Sci, Technol Eng Syst J 2020;5(3):142–9.
[32] Siohan P, Siclet C, Lacaille N. Analysis and design of OFDM/OQAM systems based on filterbank theory. IEEE Trans Signal Process 2002;50(5):1170–83.
[33] Bellanger M, Le Ruyet D, Roviras D, Terré M, Nossek J, Baltar L, Bai Q, Waldhauser D, Renfors M, Ihalainen T, et al. FBMC physical layer: a primer. Phydyas 2010;25(4):7–10.
[34] Bellanger MG. "Specification and design of a prototype filter for filter bank based multicarrier transmission," in icassp. Citeseer 2001;1:2417–20.
[35] Bölcskei H, Duhamel P, Hleiss R. Design of pulse shaping OFDM/OQAM systems for high data-rate transmission over wireless channels. In: IEEE International conference on communications, vol. 1. Institution of Electrical Engineers Inc (IEE); 1999. p. 559–64.
[36] Chen D, Qu D, Jiang T, He Y. Prototype filter optimization to minimize stopband energy with NPR constraint for filter bank multicarrier modulation systems. IEEE Trans Signal Process 2012;61(1):159–69.
[37] Chang RW. Synthesis of band-limited orthogonal signals for multichannel data transmission. Bell Syst Tech J 1966;45(10):1775–96.
[38] Le Floch B, Alard M, Berrou C. Coded orthogonal frequency division multiplex [tv broadcasting]. Proc IEEE 1995;83(6):982–96.

[39] Bölcskei H. "Orthogonal frequency division multiplexing based on offset QAM." In: Advances in Gabor analysis. Springer; 2003. p. 321–52.

[40] Farhang-Boroujeny B, Yuen C. Cosine modulated and offset QAM filter bank multicarrier techniques: a continuous-time prospect. EURASIP J Adv Signal Process 2010;2010:1–16.

[41] Proakis J, Salehi M. "Digital communications, ed. 5th; 2007.".